



# A new type of bilateral vibro-impact model: random vibration analysis

Jiamin Qian<sup>1,2</sup> · Lincong Chen<sup>1,2</sup> · Shichuan Liu<sup>1</sup>

Received: 4 December 2020 / Revised: 12 January 2021 / Accepted: 21 January 2021 / Published online: 5 February 2021  
© The Author(s), under exclusive licence to Springer-Verlag GmbH, DE part of Springer Nature 2021

## Abstract

In this work, a novel class of bilateral vibro-impact model is proposed. Unlike the traditional impact model, the energy dissipation of the novel bilateral system is measured by the model of the restitution coefficient dependent with velocity. Then the random vibration of the system is investigated in the presence of Gaussian white noise excitations. The motions of the unperturbed impact system are firstly considered and grouped into two categories. Then, the mean drift and diffusion coefficients of the two kinds of motion are calculated with the stochastic averaging methodology for energy envelope under the assumed condition that the impact vibration system is quasi-conservative. Subsequently, the probability density functions of stationary responses are computed with solving the averaged Fokker-Plank-Kolmogorov equation. Finally, two illustrations are chosen to demonstrate the reliability of the presented technique. And, the validation of analytical results is verified by the simulation data generated by Monte Carlo.

**Keywords** Bilateral vibro-impact systems · Velocity-dependent restitution coefficient · Stochastic averaging · Random vibration

## 1 Introduction

Impact vibration system is a complex nonlinear dynamical system, which has important theoretical and practical significance [1–5]. Assuming that the impact is completed in an instant, the energy dissipation is measured by the restitution coefficient. Early studies suggested that the restitution coefficient was a material dependent constant. On this basis, a great deal of researches has been carried out. Such that the non-smooth coordinate transformation techniques [6–8] are introduced, so that the traditional technique, such as stochastic averaging method [9], the path integral approach [10] and the exponential polynomial closure (EPC) method [11–13] and the iterative method of weighted residue [14] can be used to investigate impact vibration systems. In addition, Monte Carlo simulation is one of the most commonly methods for calculating the response of stochastic

impact vibration systems [15] regardless of computational efficiency and convergence. The method of generalized cell mapping was used by Wang to obtain the random response of impulsive systems [16].

However, many results [17, 18] have showed that taking the restitution coefficient as constant would reduce the accuracy of the calculation. Since then, a great deal of research has been done to modify the restitution coefficient. Johnson [19] derived the expression of the restitution coefficient of the complete plastic impact, which is then supplemented by Stronge [20]. Thornton pointed out the deficiency of Stronge model and built the expression of relative velocity of correlation of restitution coefficient [21]. While the curvature variable was not considered in Thornton's model. Refs. [22–27] modified the restitution coefficient model given by Thornton. So many researchers [28, 29] were still dedicated to studying the restitution coefficient to better reflect the energy changes in the impact process, but the existing models are either too complicated to express or cannot be verified by experiments. Recently, Ma [30] has given the modified expression of the restitution coefficient with velocity of impact, and verified it by relevant experiments.

The correction of restitution coefficient provides a new perspective for us to further explore the mechanical properties of vibro-impact system. Especially for the issue of bilateral

✉ Lincong Chen  
lincongchen@hqu.edu.cn

<sup>1</sup> College of Civil Engineering, Huaqiao University, Xiamen 361021, China

<sup>2</sup> Key Laboratory for Intelligent Infrastructure and Monitoring of Fujian Province, Huaqiao University, Xiamen 361021, China

impact, such a model can better reflect the complex energy dissipation mechanism in impact process. For this reason, a new type of bilateral impact model is developed. Currently, this kind of new bilateral impact model has not been reported. The existing research is still based on constant restitution coefficient to analyze the bilateral impact issues. For example, Dimentberg [7] investigated the response of single-degree-of-freedom (SDOF) impact model driven by random excitation with bilateral and unilateral obstacles respectively. Liu et al analyzed the random features of a two-sided impact vibration model excited by colored noise [31]. The stochastic dynamic analysis of a Duffing vibration-impact system with two side impact walls was investigated in Refs. [32, 33]. The stochastic dynamics of vibro-impact systems with distribution barriers under additive Gaussian noise excitation were reported in [34]. More recently, Su and his coworkers [35] used the stochastic averaging for energy envelope method to explore the response of the bilateral energy harvesting system.

In this work, the novel type of SDOF bilateral impact model is performed. And the random vibration of this model is analyzed. On the basis of the study of free impact vibration system, the displacement impact condition is converted to the impact condition of energy, and then the free impact vibration system can be divided according to the energy level. With the aid of stochastic averaging method for energy envelope, the mean drift and diffusion coefficients of system is calculated, by assuming that the system is quasi-conservative. The stationary probability density functions (PDFs) of system's response is calculated by solving the averaged Fokker–Plank–Kolmogorov (FPK) equation in a closed-form. As for illustration, two vibro-impact oscillations are studied, and the precision of the procedure is confirmed by the Monte Carlo simulation.

### 2 Novel type of vibro-impact system with bilateral clearance

A class of SDOF bilateral impact vibration model driven by random excitations is presented in Fig. 1. Meanwhile, the differential equation of motion reads,

$$\ddot{X} + g(X) + \varepsilon h(X, \dot{X}) = \varepsilon^{1/2} f_k(X, \dot{X}) \xi_k(t),$$

$$k = 1, 2, \dots, m, \quad |X| < \Delta, \tag{1}$$

where  $\varepsilon$  is a parameter of positive;  $g(X)$  represents the restoring force of an free vibro-impact system;  $h(X, \dot{X})$  represents damping force of linear or nonlinear;  $f_k(X, \dot{X})$  are random perturbations;  $\xi_k(t)$  mean Gaussian white noises with correlation functions  $E[\xi_k(t) \xi_l(t + \tau)] = 2D_{kl} \delta(\tau)$ ,  $k, l = 1, 2, \dots, m$ .

The impact boundary of system (1) is given below:

$$\dot{X}_+ = -e\dot{X}_-, \quad X = \pm\Delta, \tag{2}$$

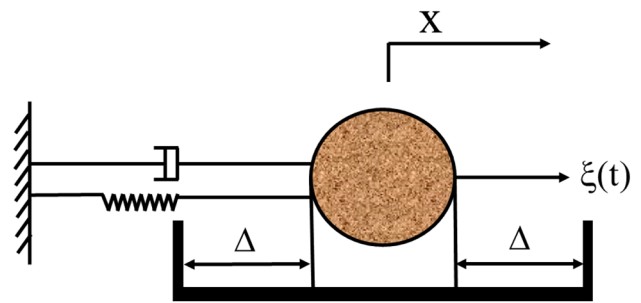


Fig. 1 Stochastic vibro-impact system with bilateral clearance

where  $\dot{X}_-$  and  $\dot{X}_+$  are rebound and impact velocities of the oscillate. The position of impact barrier is  $X = \pm\Delta$ . The coefficient of restitution is presented as a piecewise function according to the magnitude of the impact velocity, i.e.,

$$e = \begin{cases} 1 & \dot{X}_- \leq V_C \\ e(\dot{X}_-) & \dot{X}_- > V_C \end{cases}, \tag{3}$$

in which  $V_C$  is the critical velocity, which can be understood as the value of the velocity before oscillate enters the elastoplastic phase.  $e(\dot{X}_-)$  is associated with  $\dot{X}_-$ , which is constrained by the condition  $0 < e(\dot{X}_-) < 1$ .

Equation (3) suggests that the value of the restitution coefficient remains at a larger level of unity when velocity of the impact is kept below the critical velocity, which fully reflects exchange of momentum during the elastic collision phase. As velocity of the impact increases, the oscillator enters the elastoplastic impact phase. Obviously, such model is equivalent to Newton restitution coefficient to some extent [36], i.e.,  $e(\dot{X}_-) \equiv \text{constant value}$ . Recently, Ma et al. [30] considered the correlated energy dissipation due to impact and plastic deformation, and proposed the velocity-dependent restitution coefficient model as follows:

$$e(\dot{X}_-) = \omega |\dot{X}_-|^{-1/6}, \tag{4}$$

where  $\omega$  is a parameter associated with the properties of the material and is determined by the relation of  $\dot{X}_- > V_C = \omega^6$ .

### 3 Free bilateral vibro-impact system

The free bilateral vibro-impact system associated with system (1) takes form,

$$\ddot{X} + g(X) = 0, \quad |X| < \Delta,$$

$$\dot{X}_+ = -e\dot{X}_-, \quad X = \pm\Delta. \tag{5}$$

The total energy is,

$$H = \frac{1}{2}\dot{X}^2 + G(X), \tag{6}$$

where

$$G(X) = \int_0^X g(x)dx. \tag{7}$$

In the case of  $X \in (-\Delta, \Delta)$ , the period of free vibration is determined by,

$$T(H) = 2 \int_{-A}^A \frac{1}{\sqrt{2H - 2G(x)}} dx, \tag{8}$$

In which  $A < \Delta$  means the max amplitude of the mass derived by  $H = G(A)$ . Naturally, system will impact the barrier when  $H > G(\Delta)$ . Now assume that  $X = \Delta$  is the position where the first impact occurs and the corresponding total energy is,

$$H_{1-} = G(\Delta) + \frac{1}{2}\dot{X}_{1-}^2, \tag{9}$$

in which  $H_{1-}$  and  $\dot{X}_{1-}$  represents the energy of total and velocity of the free impact vibration system before impact. Thus, the total energy after impact reads,

$$H_{1+} = G(\Delta) + \frac{1}{2}\dot{X}_{1+}^2. \tag{10}$$

By combination of the Eqs. (9) and (10), the energy dissipation during this impact  $\delta_1 H$  is derived as,

$$\delta_1 H = H_{1-} - H_{1+} = [1 - e^2(\dot{X}_-)] [H_{1-} - G(\Delta)]. \tag{11}$$

Similarly, the energy loss during the impact  $\delta_2 H$  at the position  $X = -\Delta$  can be also obtained in the following form:

$$\delta_2 H = H_{2-} - H_{2+} = [1 - e^2(\dot{X}_-)] [H_{1-} - \delta_1 H - G(-\Delta)]. \tag{12}$$

Note that  $G(\Delta) = G(-\Delta)$ . Assuming that quasi-period of the impact is taken as the time interval between two impacts of the oscillator at the same obstacle  $X = \Delta$ , the total energy dissipation for a quasi-period is presented below,

$$\delta H = \delta_1 H + \delta_2 H = (1 - e^4(\dot{X}_-)) (H_{1-} - G(\Delta)), \tag{13}$$

and the quasi-period can be obtained as follows:

$$\delta(t) = 2 \int_{-\Delta}^{\Delta} \frac{1}{\sqrt{2H - 2G(x)}} dx. \tag{14}$$

### 4 Stochastic averaging of energy envelope

Introducing  $\dot{X} = Y$ , the following Itô stochastic differential equations could be derived:

$$\begin{aligned} dX &= Y dt, \\ dY &= m(X, Y)dt + \sigma(X, Y)dB(t), \quad |X| < \Delta, \end{aligned} \tag{15}$$

where,

$$m(X, Y) = -\varepsilon h(X, Y) - g(X) + \varepsilon D_{jk} f_j(X, Y) \frac{\partial}{\partial Y} f_k(X, Y), \tag{16}$$

$$\sigma^2(X, Y) = 2\varepsilon D_{jk} f_j(X, Y) f_k(X, Y). \tag{17}$$

$B(t)$  in the Eq. (15) denotes a unit Weiner process. Taking into account Eq. (15) and with the aid of Itô differential rule, the equations of Itô related to displacement  $X$  and energy  $H$  of system could be deduced as,

$$dX = \pm \sqrt{2H - 2G(X)} dt, \tag{18}$$

$$\begin{aligned} dH &= \left[ \mp \varepsilon \sqrt{2H - 2G(X)} h \left( X, \sqrt{2H - 2G(X)} \right) \right. \\ &\quad \left. + \frac{1}{2} \sigma^2 \left( X, \sqrt{2H - 2G(X)} \right) \right] dt \\ &\quad \pm \sqrt{2H - 2G(X)} \sigma \left( X, \pm \sqrt{2H - 2G(X)} \right) dW(t). \end{aligned} \tag{19}$$

By virtues of Eqs. (18) and (19), the displacement  $X(t)$  and energy  $H(t)$  are a process of rapidly varying and a process of slow process, respectively. The stochastic averaging technique of energy envelop [37] is feasible. The Itô equation of averaged related to  $H(t)$  is yielded as follows:

$$dH = \bar{m}(H)dt + \bar{\sigma}(H)dW(t), \tag{20}$$

where  $\bar{m}(H)$  denotes the mean coefficient of drift and  $\bar{\sigma}(H)$  is the mean diffusion coefficient. Note that the motion of the oscillator is grouped into two cases. One is the system will oscillate and impact alternately between the rigid barriers, the other is oscillations without impacts. Therefore, the averaged drift and diffusion coefficient could be calculated in different two cases, respectively.

#### 4.1 Case 1 $H < G(\Delta)$

In this case, the oscillate will be free of impact vibrations. The averaged drift and diffusion coefficients are:

$$\bar{m}(H) = \frac{2}{T(H)} \int_{-A}^A \left[ -\varepsilon h(X, \sqrt{2H - 2G(X)}) + \frac{1}{2} \frac{\sigma^2(X, \sqrt{2H - 2G(X)})}{\sqrt{2H - 2G(X)}} \right] dX, \tag{21}$$

$$\bar{\sigma}^2(H) = \frac{2}{T(H)} \int_{-A}^A \left[ \sqrt{2H - 2G(X)} \cdot \sigma^2(X, \sqrt{2H - 2G(X)}) \right] dX, \tag{22}$$

$$T(H) = 2 \int_{-A}^A \frac{1}{\sqrt{2H - 2G(X)}} dX. \tag{23}$$

In which  $A = G^{-1}(H)$  denotes the value of the amplitude of vibration.

### 4.2 Case 2 $H > G(\Delta)$

In such case, the system will oscillate and impact alternately between the rigid barriers. The averaged drift and diffusion coefficient can take the following forms after combining with the energy dissipation during one quasi-period,

$$\bar{m}(H) = \frac{2}{T(H)} \int_{-\Delta}^{\Delta} \left[ -\varepsilon h(X, \sqrt{2H - 2G(X)}) + \frac{1}{2} \frac{\sigma^2(X, \sqrt{2H - 2G(X)})}{\sqrt{2H - 2G(X)}} \right] dX - \frac{\delta H}{T(H)}, \tag{24}$$

$$\bar{\sigma}^2(H) = \frac{2}{T(H)} \int_{-\Delta}^{\Delta} \left[ \sqrt{2H - 2G(X)} \cdot \sigma^2(X, \sqrt{2H - 2G(X)}) \right] dX, \tag{25}$$

$$T(H) = 2 \int_{-\Delta}^{\Delta} \frac{1}{\sqrt{2H - 2G(X)}} dX. \tag{26}$$

where  $\delta H/T(H)$  indicates loss of energy during a complete impact cycle.

The Fokker-Plank-Kolmogorov equation corresponding to Eq. (20) reads,

$$\frac{\partial p}{\partial t} = -\frac{\partial}{\partial H} [\bar{m}(H)p] + \frac{1}{2} \frac{\partial^2 [\bar{\sigma}^2(H)p]}{\partial H^2}, \tag{27}$$

In which  $p = p(H, t|H_0)$  denotes the transition probability density function of energy under the condition of initial,

$$p(H, 0|H_0) = \delta(H - H_0), \tag{28}$$

and the boundary conditions,

$$\begin{aligned} p &= \text{finite}, \quad H = 0, \\ p &= 0, \partial p / \partial H = 0, \quad H \rightarrow \infty. \end{aligned} \tag{29}$$

Taking into consideration the boundary condition in Eq. (29), the solution of stationary of Eq. (27) can be calculated analytically,

$$p(H) = \frac{C}{\bar{\sigma}^2(H)} \exp \left[ \int_0^H \frac{2\bar{m}(h)}{\bar{\sigma}^2(h)} dh \right], \tag{30}$$

where  $C$  denotes a normalization constant.

The probability density of joint related to the velocity  $Y$  and the displacement  $X$  is easily deduced as

$$p(x, y) = \frac{p(H)}{T(H)} \Big|_{H=\frac{1}{2}y^2+G(x)}. \tag{31}$$

## 5 Illustrative Examples

**Example 1** The Duffing oscillator is studied. the equation of motion is described by,

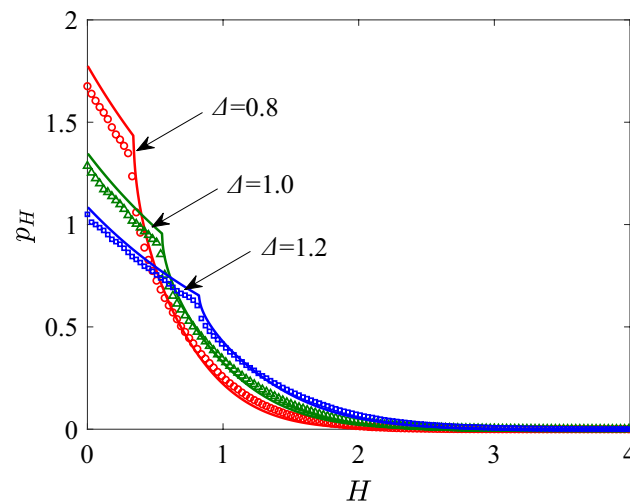


**Fig. 2** The stationary PDF of energy  $p(H)$  of system (32) for different values of the rigid barrier position under  $D=0.05$  and  $V_c=0.4$ . The other parameters are  $a=1.0$ ,  $b=0.2$ ,  $c=0.025$ . The solid lines denote the numerical results; symbols (●▲■) denote the Monte Carlo simulation of the system

$$\ddot{X} + c\dot{X} + aX + bX^3 = \xi(t), \quad |X| < \Delta \tag{32}$$

$$\dot{X}_+ = -e(\dot{X}_-)\dot{X}_-, \quad X = \pm\Delta \tag{33}$$

where  $a$  and  $b$  are constant;  $c$  represents the coefficient of damping;  $\xi(t)$  denotes the Gaussian white noise with intensity  $2D$ .

The total energy of the Eq. (32) is,

$$H = \frac{1}{2}\dot{X}^2 + G(X), \tag{34}$$

In which

$$G(X) = \frac{1}{2}aX^2 + \frac{1}{4}bX^4. \tag{35}$$

The drift and diffusion coefficients of averaged are presented below:

$$\bar{m}(H) = \begin{cases} D - \frac{2}{T(H)} \int_{-A}^A c\sqrt{2H - aX^2 - bX^4}/2dX & H < G(\Delta) \\ D - \frac{2}{T(H)} \int_{-\Delta}^{\Delta} c\sqrt{2H - aX^2 - bX^4}/2dX - \frac{\delta H}{T(H)} & H \geq G(\Delta) \end{cases}, \tag{36}$$

$$\bar{\sigma}^2(H) = \begin{cases} \frac{4D}{T(H)} \int_{-A}^A \sqrt{2H - aX^2 - bX^4}/2dX & H < G(\Delta) \\ \frac{4D}{T(H)} \int_{-\Delta}^{\Delta} \sqrt{2H - aX^2 - bX^4}/2dX & H \geq G(\Delta) \end{cases}, \tag{37}$$

$$T(H) = \begin{cases} 2 \int_{-A}^A \frac{1}{\sqrt{2H - aX^2 - bX^4}/2} dX & H < G(\Delta) \\ 2 \int_{-\Delta}^{\Delta} \frac{1}{\sqrt{2H - aX^2 - bX^4}/2} dX & H \geq G(\Delta) \end{cases}, \tag{38}$$

where  $A = [((a^2 + 4bH)^{0.5} - a)/b]^{0.5}$ .

Figures 2, 3, 4, 5, 6, 7, 8, 9, 10, 11 show the numerical results and the direct Monte Carlo simulation’s data of stationary response of Eq. (32). In Fig. 2, the stationary PDFs of energy  $H$  for different positions of rigid barrier are presented, respectively. It is seen that the peak value of the stationary PDF of energy of the system decreases with the increase of the rigid barrier position, and the rate of decay of the PDF decreases correspondingly. Furthermore, Figs. 3, 4, 5 demonstrate the corresponding joint PDFs for the velocity  $Y$  and displacement  $X$ , respectively.

Figure 6 demonstrates the influence of the yield velocity on the system. It can be seen that a larger yield velocity  $V_C$  corresponds to a smaller energy peak, which implies that an increased amount of the energy is dissipated with the increase of yield velocity  $V_C$ . Similarly, the joint PDFs derived by the presented technique and Monte Carlo simulation results, respectively are also shown, see Figs.7, 8, 9. It is worth pointing out that Figs. 8 and 9 are almost indistinguishable. This means that as the yield velocity increases, the difficulty of system collision will increase so that the system is in the elastic impact stage or no impact occurs.

Moreover, the effect of the excitation intensities on the system is displayed in Fig. 10 and the discussion on the damping coefficient is exhibited in Fig. 11. Finally, it is diverting to note that due to the constraint of the rigid barrier

**Fig. 3** The joint probability density of displacement and velocity of system (32) with  $\Delta=0.8$  under  $D=0.05$  and  $V_C=0.4$ . The other parameters are the same as those in Fig. 2. **a** denotes the analytical result, and **b** denotes the Monte Carlo simulation result

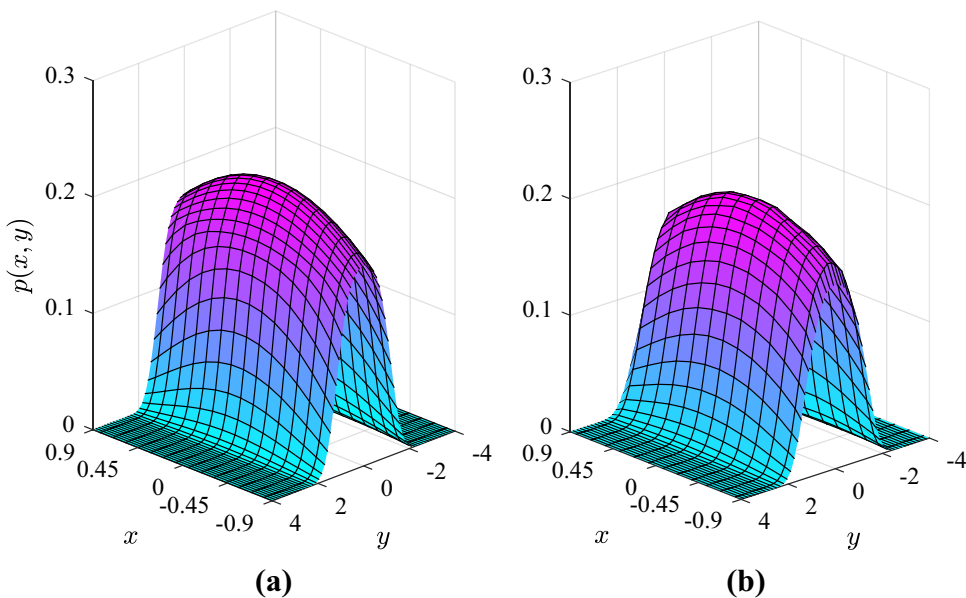


**Fig. 4** The joint probability density of displacement and velocity of system (32) with  $\Delta = 1.0$  under  $D = 0.05$  and  $V_C = 0.4$ . The other parameters are the same as those in Fig. 2. **a** denotes the analytical result, and **b** denotes the Monte Carlo simulation result

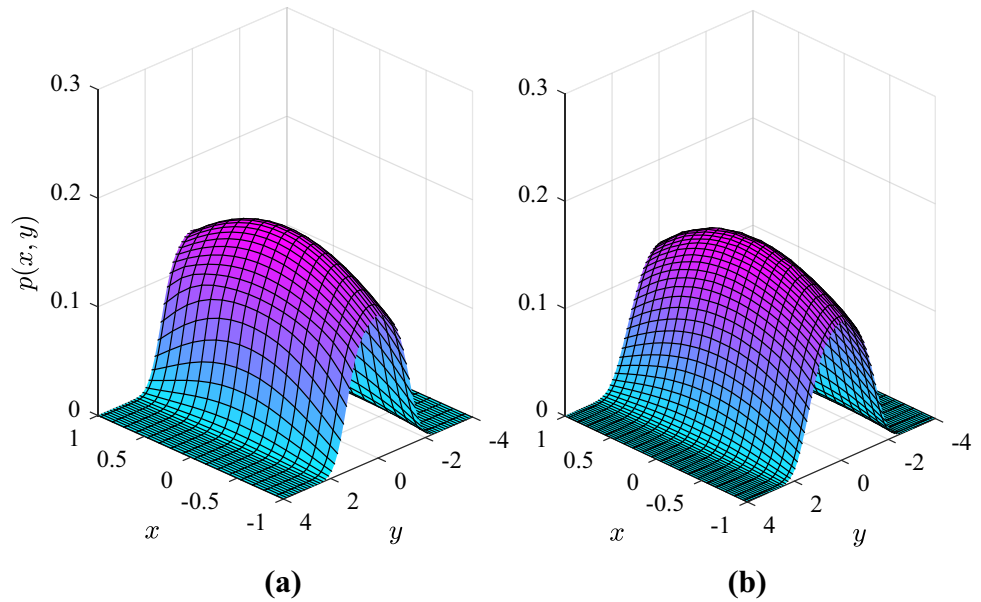
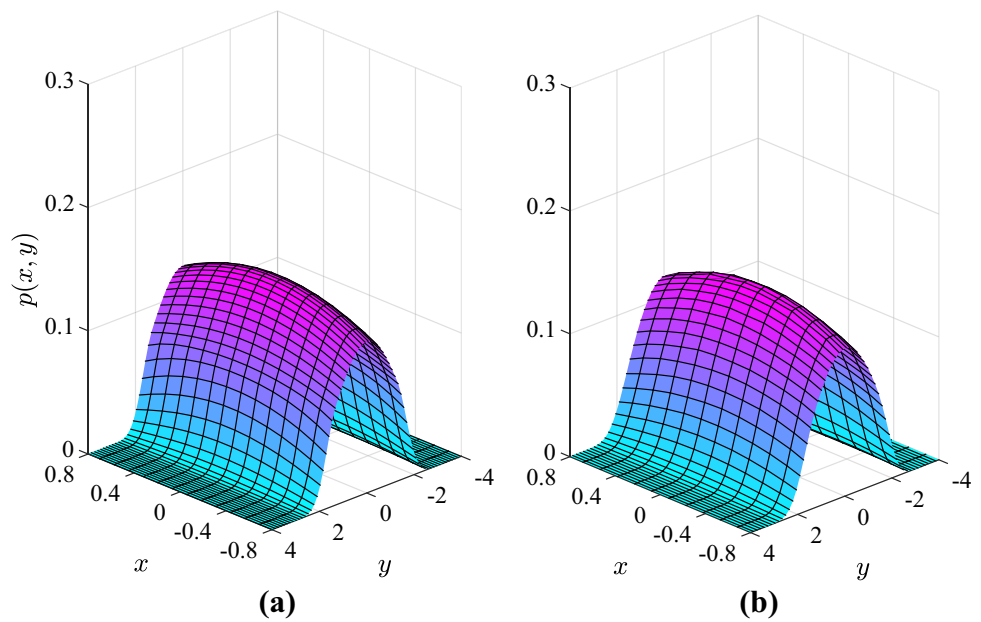


**Fig. 5** The joint probability density of displacement and velocity of system (32) with  $\Delta = 1.2$  under  $D = 0.05$  and  $V_C = 0.4$ . The other parameters are the same as those in Fig. 2. **a** denotes the analytical result, and **b** denotes the Monte Carlo simulation result



position, the stationary PDFs of energy are both show inflexion points, the position of which are located at  $H = G(\Delta)$ . Since  $G(\Delta)$  is only related to  $\Delta$ , the inflexion in Fig. 2 moves to the larger energy  $H$  with the increase of  $\Delta$ .

**Example 2** As the second illustration, Duffing-van der pol impact vibration system is considered. The differential equation of motion is written as,

$$\ddot{X} + (c_1 - c_2 X^2)\dot{X} + aX + bX^3 = \xi(t), \quad |X| < \Delta, \quad (39)$$

$$\dot{X}_+ = -e(\dot{X}_-)\dot{X}_-, \quad X = \pm\Delta, \quad (40)$$

where  $c_1$  and  $c_2$  represent the coefficient of damping;  $\xi(t)$  denotes the Gaussian white noise with intensity  $2D$ . The total energy of the Eq. (39) is the same as those in Eq. (34). The potential energy is the same as Eq. (35).

The mean drift and diffusion coefficients for this example are given below:



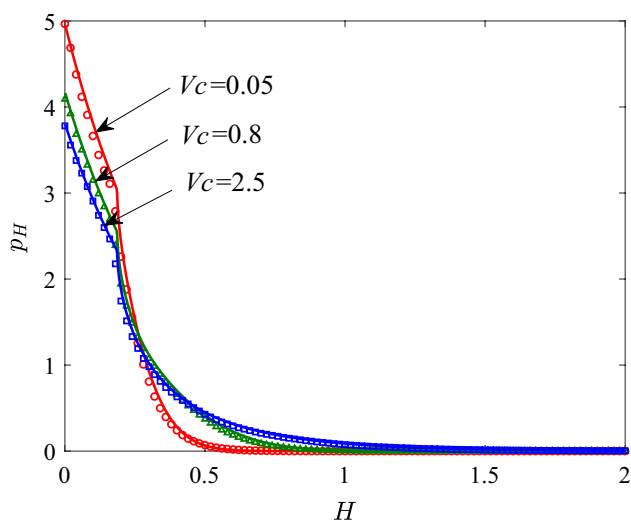


**Fig. 6** The stationary PDF of energy  $p(H)$  of system (32) for different values of yield velocity under  $D=0.01$  and  $V_C=0.6$ . The other parameters are  $a=1.0$ ,  $b=0.2$ ,  $c=0.025$ . The solid lines denote the numerical results; symbols (●▲■) denote the Monte Carlo simulation of the system

$$\bar{\sigma}^2(H) = \begin{cases} \frac{4D}{T(H)} \int_{-A}^A \sqrt{2H - aX^2 - bX^4/2} dX & H < G(\Delta) \\ \frac{4D}{T(H)} \int_{-\Delta}^{\Delta} \sqrt{2H - aX^2 - bX^4/2} dX & H \geq G(\Delta) \end{cases}, \tag{42}$$

$$T(H) = \begin{cases} 2 \int_{-A}^A \frac{1}{\sqrt{2H - aX^2 - bX^4/2}} dX & H < G(\Delta) \\ 2 \int_{-\Delta}^{\Delta} \frac{1}{\sqrt{2H - aX^2 - bX^4/2}} dX & H \geq G(\Delta) \end{cases}, \tag{43}$$

The numerical results of stationary response of system (39) are demonstrated in Figs.12, 13, 14, 15, 16. Meanwhile, the direct Monte Carlo simulation result is supplied for examining the reliability of the proposed method. In Figs. 12, 13, 14, the effect of velocity of yield  $V_C$ , noise intensities  $D$  and rigid barrier position  $\Delta$  onto the PDFs of stationary are examined, respectively. It can be conducted from those figures that there is a good coincidence between the Monte Carlo simulation results and the analytical solutions.

$$\bar{m}(H) = \begin{cases} D - \frac{2}{T(H)} \int_{-A}^A (c_1 - c_2 X^2) \sqrt{2H - aX^2 - bX^4/2} dX & H < G(\Delta) \\ D - \frac{2}{T(H)} \int_{-\Delta}^{\Delta} (c_1 - c_2 X^2) \sqrt{2H - aX^2 - bX^4/2} dX - \frac{\delta H}{T(H)} & H \geq G(\Delta) \end{cases}, \tag{41}$$

**Fig. 7** The joint probability density of displacement and velocity of system (32) with  $V_C=0.05$  under  $D=0.01$  and  $\Delta=0.6$ . The other parameters are the same as those in Fig. 6. **a** denotes the analytical result, and **b** denotes the Monte Carlo simulation result

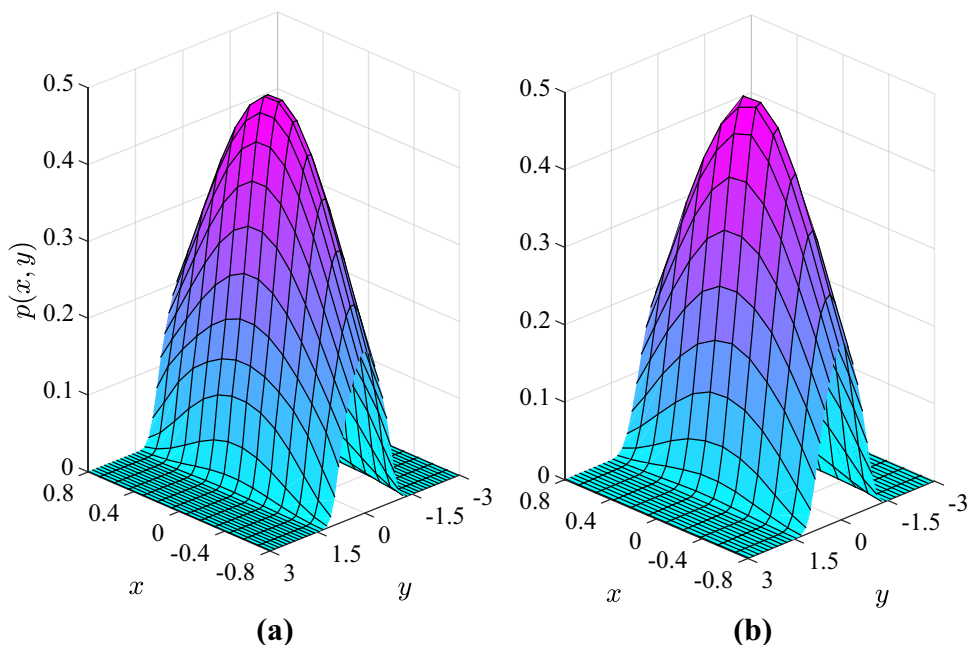


**Fig. 8** The joint probability density of displacement and velocity of system (32) with  $V_C=0.8$  under  $D=0.01$  and  $\Delta=0.6$ . The other parameters are the same as those in Fig. 6. **a** denotes the analytical result, and **b** denotes the Monte Carlo simulation result

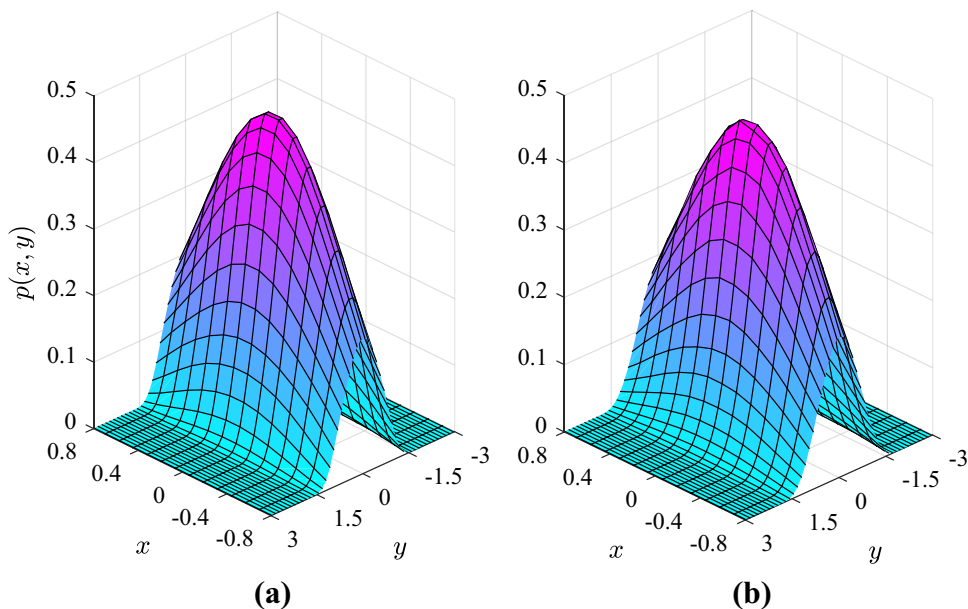
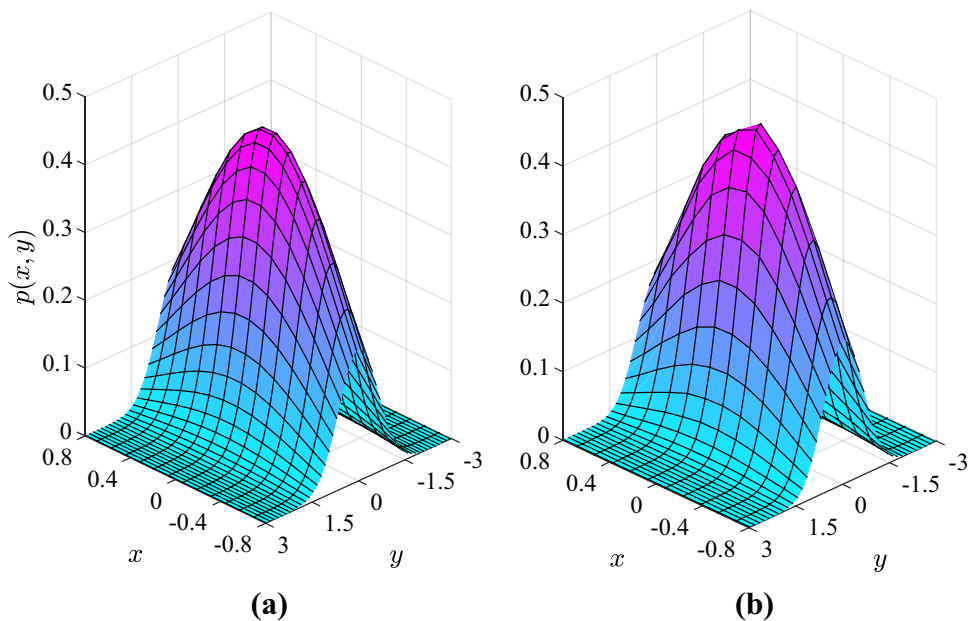


**Fig. 9** The joint probability density of displacement and velocity of system (32) with  $V_C=2.5$  under  $D=0.01$  and  $\Delta=0.6$ . The other parameters are the same as those in Fig. 6. **a** denotes the analytical result, and **b** denotes the Monte Carlo simulation result



As an additional illustration, the PDFs of joint of the velocity  $y$  and displacement  $x$  from theoretical results are displayed in Figs. 15 and 16 when the rigid barrier at  $\Delta = 3.0$  and  $\Delta = 1.0$ , respectively. In contrast to Figs. 15 and 16, it is clearly observed that the system has no impact when the rigid barrier position is very large, and the PDFs of the system with respect to energy present a complete limit cycle. However, the limit cycle displays incomplete due to the impact of the system as the impact boundary gets closer and closer to the oscillator. According to the definition of stochastic P-bifurcation, the disappearance and appearance

of complete limit cycle due to the change of system's parameter is a stochastic P-bifurcation.

## 6 Conclusion

In this letter, the random vibration of the novel bilateral model driven by Gaussian white noise excitation is analyzed. By studying the unperturbed vibration system, the motion state of the system is divided into free vibration and impact vibration. The mean drift and diffusion



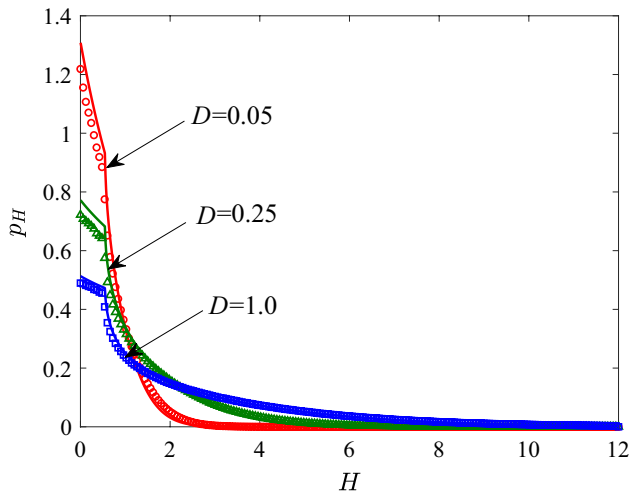


**Fig. 10** The stationary PDF of energy  $p(H)$  of system (32) for different values of noise intensities under  $\Delta=1.0$  and  $V_C=0.6$ . The other parameters are  $a=1.0$ ,  $b=0.2$ ,  $c=0.025$ . The solid lines denote the numerical results; symbols (●▲■) denote the Monte Carlo simulation of the system

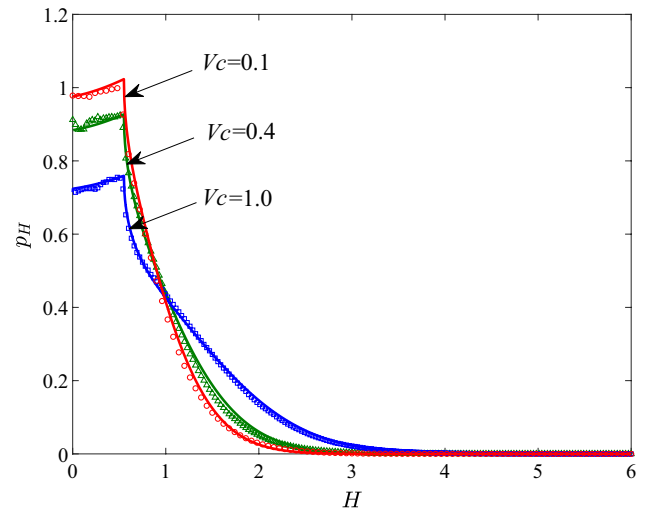


**Fig. 12** The stationary PDF of energy  $p(H)$  of system (39) for different values of yield velocity under  $\Delta=1.0$  and  $V_C=0.4$ . The other parameters are  $a=1.0$ ,  $b=0.2$ ,  $c_1=-0.01$ ,  $c_2=0.005$ . The solid lines denote the numerical results; symbols (●▲■) denote the Monte Carlo simulation of the system

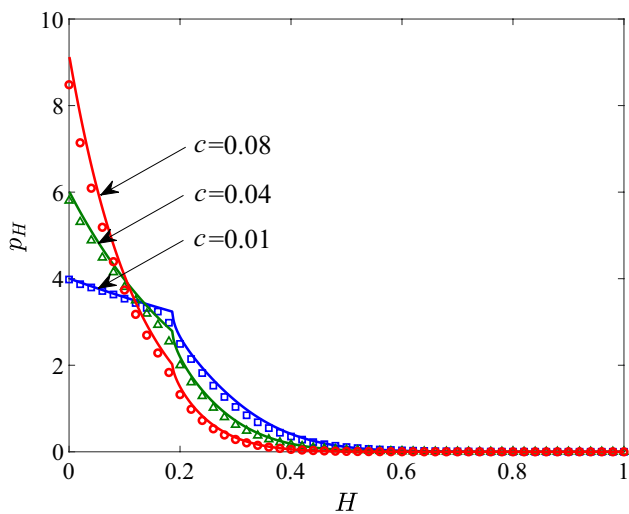


**Fig. 11** The stationary PDF of energy  $p(H)$  of system (32) for different values of damping coefficient under  $\Delta=1.0$ ,  $V_C=0.05$  and  $D=0.01$ . The other parameters are  $a=1.0$ ,  $b=0.2$ . The solid lines denote the numerical results; symbols (●▲■) denote the Monte Carlo simulation of the system

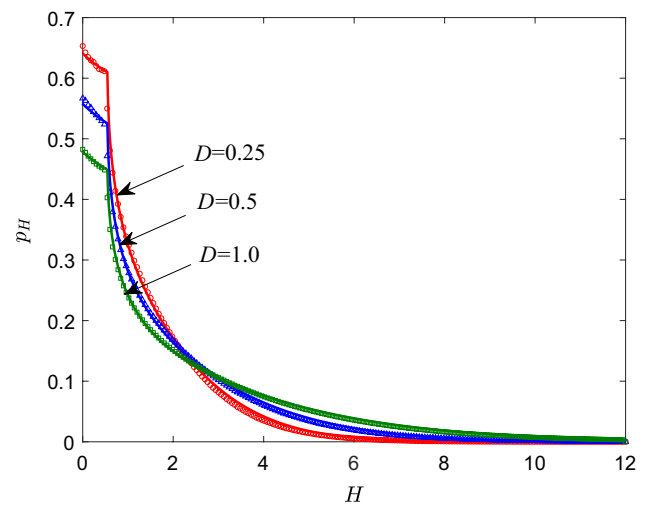


**Fig. 13** The stationary PDF of energy  $p(H)$  of system (39) for different values of noise intensities under  $\Delta=1.0$  and  $V_C=0.4$ . The other parameters are  $a=1.0$ ,  $b=0.2$ ,  $c_1=-0.01$ ,  $c_2=0.005$ . The solid lines denote the numerical results; symbols (●▲■) denote the Monte Carlo simulation of the system

coefficients under two different motion states are obtained by means of the stochastic average method of energy envelope, whereafter the stationary response of the system is calculated by solving the corresponding averaged FPK equation. Two illustrations are given to the effectiveness

of the performed technique and the influence of several critical parameters on the system is examined. All numerical results could be conducted that the analytical solution with proposed method is consistent with the direct Monte Carlo simulation data.

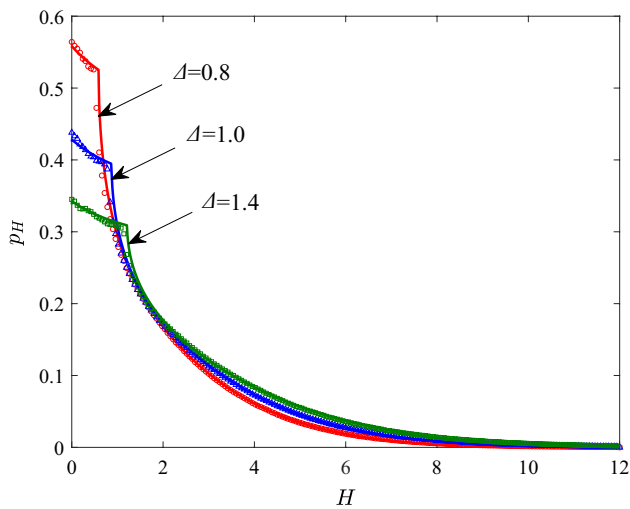


**Fig. 14** The stationary PDF of energy  $p(H)$  of system (39) for different values of the rigid barrier under  $V_C=0.4$  and  $D=0.5$ . The other parameters are  $a=1.0$ ,  $b=0.2$ ,  $c_1=-0.01$ ,  $c_2=0.005$ . The solid lines denote the numerical results; symbols (●▲■) denote the Monte Carlo simulation of the system  $\Delta$

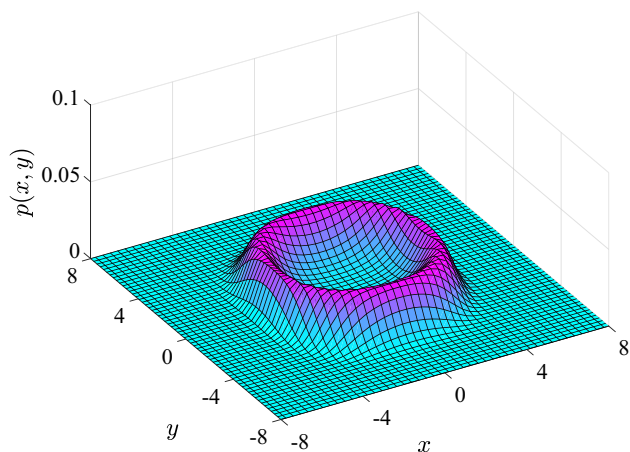


**Fig. 15** The analytical joint probability density of displacement and velocity of system (39) with  $\Delta=3.0$  under  $D=0.01$  and  $\Delta=0.6$ . The other parameters are the same as those in Fig. 14

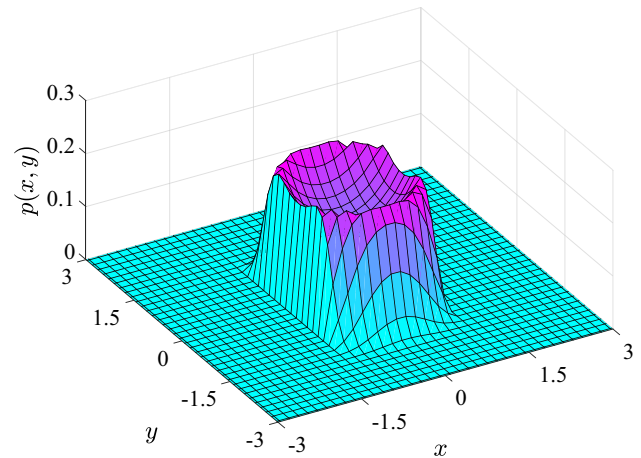


**Fig. 16** The analytical joint probability density of displacement and velocity of system (39) with  $\Delta=1.0$  under  $D=0.01$  and  $\Delta=0.6$ . The other parameters are the same as those in Fig. 14

**Author contributions** JQ: Investigation, Data curation, Writing—original draft. LC: Conceptualization, Methodology, Supervision, Project administration. SL: Data Collation, textual corrigendum.

**Funding** The National Natural Science Foundation of China (No. 11672111, No. 12072118), the Program for New Century Excellent Talents in Fujian Province University, the Natural Science Foundation of Fujian Province of China (No. 2019J01049).

**Code availability** The code that support the findings of this study are available from the corresponding author upon reasonable request.

### Compliance with ethical standards

**Conflicts of interest** The authors declare that they have no conflict of interest.

**Availability of data and material** The data and material that support the findings of this study are available from the corresponding author upon reasonable request.

### References

1. Dimentberg MF, Iourtchenko DV (1999) Towards incorporating impact losses into random vibration analyses: a model problem. *Probabilistic Eng Mech* 14:323–328

2. Ibrahim RA (2009) *Vibro-impact dynamics: modeling, mapping and applications*. Springer, Berlin
3. Kecik K, Brzeski P, Perlikowski P (2016) Non-linear dynamics and optimization of a harvester-absorber system. *Int J Struct Stab Dyn* 17:1740001
4. Liu WB, Dai HL et al (2017) Suppressing wind-induced oscillations of prismatic structures by dynamic vibration absorbers. *Int J Struct Stab Dyn* 17:1750056
5. Pratiknyo YB, Setiawan R, Suweca IW (2019) Experimental and theoretical investigation of combined expansion tube-axial splitting as impact energy absorbers. *Int J Struct Stab Dyn* 20:2050021
6. Zhuravlev VF (1976) A method for analyzing vibration-impact systems by means of special functions. *Mech Solids* 11:23–27
7. Dimentberg M, Menyailov A (1979) Response of a single-mass vibroimpact system to white-noise random excitation. *ZAMM - J Appl Math Mech* 59:709–716
8. Ivanov AP (1994) Impact oscillations: linear theory of stability and bifurcations. *J Sound Vib* 178:361–378
9. Xu W, Li C, Yue X, Rong H (2016) Stochastic responses of a vibro-impact system with additive and multiplicative colored noise excitations. *Int J Dyn Control* 4:393–399
10. Dimentberg MF, Iourtchenko DV (2004) Random vibrations with impacts: a review. *Nonlinear Dyn* 36:229–254
11. Er G-K (1998) An improved closure method for analysis of nonlinear stochastic systems. *Nonlinear Dyn* 17:285–297
12. Zhu HT (2015) Stochastic response of a vibro-impact Duffing system under external Poisson impulses. *Nonlinear Dyn* 82:1001–1013
13. Zhu HT (2015) Stochastic response of a parametrically excited vibro-impact system with a nonzero offset constraint. *Int J Dyn Control* 4:180–194
14. Chen L, Qian J, Zhu H, Sun J (2019) The closed-form stationary probability distribution of the stochastically excited vibro-impact oscillators. *J Sound Vib* 439:260–270
15. Yurchenko D, Song L (2006) Numerical investigation of a response probability density function of stochastic vibroimpact systems with inelastic impacts. *Int J Non Linear Mech* 41:447–455
16. Wang L, Ma S, Sun C et al (2018) The stochastic response of a class of impact systems calculated by a new strategy based on generalized cell mapping method. *J Appl Mech* 85:54502
17. Kecskemethy A, Lüder J (1996) Rigid and elastic approaches for the modeling of collisions with friction in multibody systems. *Zeitschrift für Angew Math und Mech* 76:243–244
18. Wang Y, Mason MT (1992) Two-Dimensional Rigid-Body Collisions With Friction. *J Appl Mech* 59:635
19. Johnson KL (1985) *Contact Mechanics*. In: Cambridge, UK: Cambridge University Press
20. Stronge WJ (1995) Theoretical coefficient of restitution for planar impact of rough elasto-plastic bodies. *Am Soc Mech Eng Appl Mech Div AMD* 205:351–362
21. Thornton C (1997) Coefficient of restitution for collinear collisions of elastic-perfectly plastic spheres. *J Appl Mech Asme* 64:383–386
22. Mesarovic SD, Fleck NA (1999) Spherical indentation of elastic-plastic solids. *Proc Math Phys Eng ences* 455:2707–2728
23. Vu-Quoc L, Zhang X (2000) A normal force-displacement model for contacting spheres accounting for plastic deformation: force-driven formulation. *J Appl Mech* 67:363–371
24. Kogut L, Etsion I (2002) Elastic-plastic contact analysis of a sphere and a rigid flat. *J Appl Mech* 69:657–662
25. Zhang X, Vu-Quoc L (2002) Modeling the dependence of the coefficient of restitution on the impact velocity in elasto-plastic collisions. *Int J Impact Eng* 27:317–341
26. Weir G, McGavin P (2008) The coefficient of restitution for the idealized impact of a spherical, nano-scale particle on a rigid plane. *Proc R Soc A Math* 464:1364–5021
27. Etsion I, Kligerman Y, Kadin Y (2005) Unloading of an elastic-plastic loaded spherical contact. *Int J Solids Struct* 42:3716–3729
28. Kharaz AH, Gorham DA (2000) A study of the restitution coefficient in elastic-plastic impact. *Philos Mag Lett* 80:549–559
29. Minamoto H, Kawamura S (2011) Moderately high speed impact of two identical spheres. *Int J Impact Eng* 38:123–129
30. Ma D, Liu C (2015) Contact law and coefficient of restitution in elastoplastic spheres. *J Appl Mech* 82:121006–121015
31. Liu D, Li J, Meng Y (2019) Probabilistic response analysis for a class of nonlinear vibro-impact oscillator with bilateral constraints under colored noise excitation. *Chaos Solitons Fractals* 122:179–188
32. Kumar P, Narayanan S, Gupta S (2016) Bifurcation analysis of a stochastically excited vibro-impact Duffing-Van der Pol oscillator with bilateral rigid barriers. *Int J Mech ences* 127:103–117
33. Yang G, Xu W, Gu X, Huang D (2016) Response analysis for a vibroimpact Duffing system with bilateral barriers under external and parametric Gaussian white noises. *Chaos Solitons Fractals* 87:125–135
34. Chen L, Zhu H, Sun JQ (2019) Novel method for random vibration analysis of single-degree-of-freedom vibroimpact systems with bilateral barriers. *Appl Math Mech* 40:1759–1776
35. Su M, Xu W, Zhang Y, Yang G (2021) Response of a vibro-impact energy harvesting system with bilateral rigid stoppers under Gaussian white noise. *Appl Math Model* 89:991–1003
36. Qian J, Chen L (2021) Random vibration of SDOF vibro-impact oscillators with restitution factor related to velocity under wide-band noise excitations. *Mech Syst Signal Process* 147:107082
37. Zhu W, Lin YK (1905) stochastic averaging of energy envelope. *J Eng Mech* 117:1890–1905